Macromolecules
ARTICLE

Macromolecules **2010**, *43*, 3487–3501 **3487**
DOI: 10.1021/ma902701z

Theory of Self-Assembling Structures of Model Oligopeptides

A. N. Semenov*,†,‡ and A. V. Subbotin†,‡

†*Institut Charles Sadron, CNRS-UPR 22, Université de Strasbourg, 23 rue du Loess, BP 84047, 67034 Strasbourg Cedex 2, France, and* ‡*Institute of Petrochemical Synthesis, Russian Academy of Sciences, Moscow, 119991, Russia*

Received December 9, 2009; Revised Manuscript Received February 4, 2010

ABSTRACT: Aggregation and micelle formation in dilute solutions of amphiphilic oligopeptides (Ala_{nH} Asp_{nP}) is considered theoretically. It is shown that the peptides can self-assemble forming micelles of different morphologies in the regime where Asp units are negatively charged. The micelles are stable thermodynamically if a sufficient amount of monovalent salt is added (the "salting in" effect). The thermodynamic stability of the micelles also strongly depends on pH and on the size δ of added cations. The micelles get destabilized as their surface charge (due to Asp units) decreases at low pH or low ionic strength I_∞. A larger cation size δ also results in aggregation (precipitation) of the micelles. The aggregation process can be kinetically arrested due to electrostatic repulsion even in the regime of weakly charged Asp units. The kinetically defined size R of the aggregates strongly depends on the effective peptide/water interfacial tension γ and on the Debye length r_D: R decreases as either γ or r_D is increased.

1. Introduction

It is well-known that protein molecules often assume compact robust conformations (a collapsed molten globule or a specific three-dimensional structure of a native state).[1] Native protein globules are stable and do not precipitate; these features are important for many biological processes (e.g., enzymatic activities). In some cases, however, proteins have a tendency to aggregate and form various self-assembling structures instead of separate globules. The aggregation can play important positive roles in biosystems (collagen or actin fibrils, microtubules, etc.),[2,3] but it can also lead to undesirable structures (amyloid fibrils, prions) resulting from a protein misfolding.[4−6]

An important challenge is to find a relationship between the structure of protein assemblies (fibrils, micelles) and the primary structure of the protein molecule (the aminoacid sequence) together with the solution conditions. This general problem seems to be extremely difficult. Trying to shed some light on it, we chose to analyze self-assembly in simpler model systems: aqueous solutions of rather short identical oligopeptides. Such systems are also interesting in their own right since peptide assemblies play important roles both for biological processes[7] and in technological and biomedical applications.[8−12]

The peptides considered mostly in the present paper involve just two types of aminoacid residues: alanine (Ala) and aspartic acid (Asp). The peptides are strongly amphiphilic as Ala is hydrophobic, and Asp is hydrophilic (it is polar and charged in a wide range of conditions). Such peptides can form aggregated core−shell structures in water. We focus on the Ala-Asp copolymers with the same molecular weight and composition, [Asp:Ala] = n_P:n_H with $n_P = 2$ and $n_H = 24$ (see Figure 1 where each open circle represents three Ala units). It is assumed that the condensed hydrophobic core is amorphous. The present theory is therefore not applicable to aggregates with crystalline or semicrystalline cores. The choice of the Ala and Asp units is arbitrary to some extent. In principle, the general theory developed in this paper is applicable to many systems of oligopeptide copolymers involving neutral and charged units whose molecular structure can be described in terms of a few basic essential parameters including the interaction energies, the degree of charging and geometrical parameters of aminoacid units.

We find that self-assembling properties of these peptides strongly depend on the sequence. On the other hand, our analysis shows that high amphiphilicity as such does not guarantee formation of well-defined thermodynamically stable soluble micelles. It is predicted, however, that the studied oligopeptides can form kinetically stable finite aggregates whose size depends on the Debye screening length r_D and other solution parameters. We also reveal some general features of the kinetic stabilization of peptide assemblies.

2. The Model Systems and the Free Energy

2.1. The Model. Let us consider aqueous solutions of relatively short peptide molecules consisting of two kinds of monomer units, Ala and Asp. The examples of such 26-residue peptides with four distinct chemical sequences (marked as P1, ..., P4) are shown in Figure 1. In the more general case the molecules consist of n_H Ala-units and n_P Asp-units ($n_H = 24$ and $n_P = 2$ in Figure 1); the P1 structure is telechelic with two Asp units at the ends, P2 is diblock copolymer Ala_{n_H}-Asp_{n_P}, etc.

Hydrophilic Asp units are polar and charged, so their interactions are controlled by pH and ionic strength. Hydrophobic Ala units are neutral; their interactions are temperature sensitive. The model peptides therefore possess one of the main properties of proteins, the amphiphilicity, which is also inherent in surfactants (both low-molecular[13] and block copolymer[14,15]) and polyelectrolytes.[19−22] It must therefore be expected that the Ala-Asp peptides have a tendency for formation of micellar structures involving an Ala core protected by Asp units located at the Ala/water interface. Specific interactions of Ala units in the hydrophobic core may or may not result in a periodic ordered (crystalline) core structure. We assume, for simplicity, that the core is free from any crystalline regions, i.e., that it is entirely

*Corresponding author.

Published on Web 03/10/2010

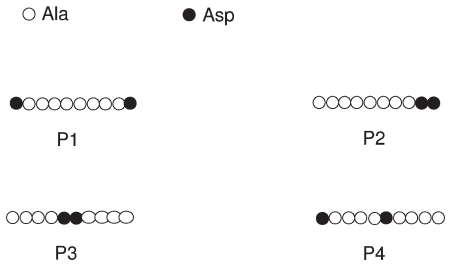

Figure 1. $Ala_{nH}Asp_{nP}$ peptides with $n_H = 24$ alanine (Ala) units and $n_P = 2$ aspartic acid (Asp) units. Each open circle corresponds to 3 Ala units. The number of Asp "blocks" is $n_{Pb} = 2$ for P1 and P4, and $n_{Pb} = 1$ for P2 and P3 structures.

amorphous. This is not impossible in view of the reports that short Ala-homopeptides tend to adopt random-coil conformations in aqueous environments.[37,38] The coil conformations may define (perhaps, metastable) disordered amorphous internal structure of aggregates formed by Ala-Asp peptides in aqueous solution (see also the Discussion, point 7 of section 7).[39]

The Ala/water interfacial energy depends on the surface concentration σ of Asp units in a nonmonotonic way: the energy is increasing both for low and large surface concentrations of hydrophilic units (at low σ the effect is due to unfavorable Ala/water contacts, at high σ it is due to Asp/Asp repulsion). Thus, there is some preferred surface concentration defining the optimal surface area of the aggregate (proportional to the total number of Asp units). This selected surface area essentially defines the micellar geometry as shown below.

The energy penalty for an Asp unit located inside the Ala core is typically high in the regime of interest (where micelles are formed at all, see section 5). It is therefore reasonable to assume that most Asp units are located at the peptide/water interface. This condition implies that Ala-fragments must be extended away from the surface inside the core. Generally, poly-Ala chains show various conformations defined by intra- and intermolecular H-bonding, involving α-helical or β-sheet motifs (including β-hairpins and β-bends) depending on the environment; β-structures dominate in the case of shorter chains, in more polar environments and at higher temperatures.[41,37] β-structures are rather compatible with random-coil conformations;[37] such conformations must be therefore anticipated in disordered amorphous aggregates (micelle cores) of oligomeric poly-Ala. A short Ala-chain with $n_H \sim 20$ can be stretched rather easily (see the next section), hence the core size along the direction normal to the surface must be defined by the maximum extension length of the Ala-fragment.

2.2. The Free Energy. A micellar aggregated structure can be described basically in terms of amorphous hydrophobic domains (aggregates of hydrophobic Ala units) and interfaces stabilized by hydrophilic (Asp) units. Accordingly, the free energy of a micelle can be written as (cf. the theoretical approach of ref 23)

$$F \approx F_{core} + F_{loc} + F_s + F_{bend} + F_{el} \qquad (1)$$

Here and below $F = \mathscr{F}/Q$ is free energy per peptide molecule with n_H Ala monomers and n_P Asp units ($\mathscr{F}$ is the total free energy, Q is the aggregation number). The terms in the rhs account, respectively, for the following: (i) the bulk of Ala−core; (ii) the entropy of localization of Asp units on the surface; (iii) the surface energy (including the Coulomb interactions); (iv) the energy contribution due to surface bending; (v) the conformational elastic energy of Ala blocks.

$F_{core} = -n_H\varepsilon_H$ in eq 1 is the free energy gained upon aggregation of Ala fragments. The energy ε_H (the effective energy of attraction per Ala monomer) depends on temperature T, but it is assumed to be independent of the micelle geometry since the core is characterized by disordered amorphous internal structure. We also assume that the density ρ_0 inside the micelle is independent of the micellar geometry and is nearly equal to the density of undiluted poly-alanine, $\rho_0 \approx 1.3$ g/cm^3.[24] Hence, the micelle volume V per peptide molecule is also fixed: $V = V^* = (M_{1H}n_H + M_{1P}n_P)/(\rho_0 N_A)$ ($M_{1H} = 71$, $M_{1P} = 115$ are molecular weights of Ala and Asp units, respectively; N_A is Avogadro's number).

The free energy F_{loc} corresponds to the ideal-gas entropy of localization of Asp groups at the interface,

$$F_{loc} \simeq k_B T n_{Pb} \ln\frac{V^*}{A\Delta} \qquad (2)$$

where Δ is the interfacial thickness, A is the interfacial area (per peptide), and n_{Pb} is the number of Asp "blocks" in the peptide molecule ($n_{Pb} = 2$ for peptides P1 and P4, and $n_{Pb} = 1$ for P2 and P3).

F_s is the free energy of the plane peptide/water interface. It depends on the surface area A per peptide molecule and on the surface concentration σ of polar (Asp) units:

$$F_s = A[\gamma_0 + f_{int}(\sigma)] \qquad (3)$$

where γ_0 is the surface tension at the Ala/water interface (in the absence of Asp units), σ is the number of Asp units per unit interfacial area (surface concentration of Asp units), and f_{int} is the free energy of interactions between charged Asp units at the surface including the free energy of proton dissociation (from carboxylic groups), the electrostatic interactions of counterions in the diffuse screening layer near the surface and the entropy of their redistribution. Below we will largely consider the regime when nearly all Asp units are located at the surface. In this case $\sigma = n_P/A$, hence the minimum of F with respect to A defines both the optimum interfacial area A^* and the optimum surface concentration of Asp units $\sigma^* = n_P/A^*$.

F_{bend} is the free energy contribution due to the interfacial curvature. For small curvatures the elastic bending energy can be approximated by the Helfrich expression:

$$F_{bend} \simeq A\left(-\kappa C + \frac{1}{2}KC^2 + K_G C_1 C_2\right) \qquad (4)$$

where $C = C_1 + C_2$ is the sum of the two principal curvatures C_1, C_2 ($C > 0$ for convex interface, e.g. for a spherical micelle), K is the mean bending modulus, K_G is Gaussian bending modulus and κ is another elastic constant reflecting an asymmetry of the interface (Ala units inside and Asp units and ions outside). It is important that κ is positive and large due to strong lateral repulsion of ions in the electrical double layer (Gouy−Chapman layer[25]) favoring convex surface of the peptide aggregate. Therefore, F_{bend} decreases as $C > 0$ is increased; this monotonic decrease persists up to high curvatures $C \sim C^* \gg 1/L$, where L is the peptide length.[16]

Finally, F_{el} is the conformational elastic energy of Ala-blocks that are anchored to the micelle surface by Asp groups, and are elongated away from the surface toward the micelle core center, $F_{el} = \langle U_{el}\rangle$, where U_{el} is the elastic energy of elongated Ala-blocks in a peptide and $\langle\cdot\rangle$ means averaging over all molecules. The conformational statistics of Ala-oligopeptides with polymerization degree $n_H = 5 \div 20$ was studied in ref 42 by Monte Carlo modeling. They found

that end-to-end distance r distribution is markedly non-Gaussian for peptides with $n_H = 10 \div 20$: the distribution is strongly asymmetric and its maximum is significantly shifted toward extended chains (see Figure 3a in ref 42). The function $f(r)$ shown in this figure is related to the elastic energy $U_{el}(r)$: $f(r) = \text{const}\ r^2 e^{-U_{el}(r)/(k_BT)}$. The elastic energy $U_{el}(r)$ obtained from the data[42] for $n_H = 20$ shows a weak variation ($\Delta U_{el} \lesssim k_BT$) for $0.15r_{max} \lesssim r \lesssim 0.75r_{max}$, where $r_{max} = L = n_H l_1$ defines the maximum chain end-to-end ($l_1 \approx 3.6$ Å is the main-chain contour length per amino acid residue).[26] The typical elastic energy variation $\Delta F_{el} \lesssim k_BT$ is small compared with other free energy contributions (of many k_BT per chain), in particular, those due to the electrostatic interactions of Asp units (see the end of section 4.1). The Ala blocks with $n_H \sim 20$ can thus be easily stretched almost up the maximum allowed length r_{max} due to the electrostatic effects that often strongly favor larger core size. To simplify the model, in what follows we adopt the following simple approximation: $U_{el}(r) = 0$ for $r < r_{max}$, $U_{el}(r) = \infty$ for $r > r_{max}$. In other words, we neglect the conformational energy F_{el} of Ala-blocks simply replacing its effect by the condition $r < r_{max}$.

The micelle structure is therefore essentially defined by the surface effects and by the geometrical packing (density) restrictions applied to its hydrophobic core.

3. The Interfacial Energy

3.1. Coulomb Effects. An Asp unit can be either neutral (with polarized $COO^- H^+$ group) or charged (with COO^- anion and dissociated proton). Let us denote the energy difference between the neutral (0) and charged (1) states as $\Delta E = E_1 - E_0$. ΔE depends on interactions of an Asp unit with the surrounding molecules, i.e. it depends on the environment. This dependence is pronounced: the energy of a charged Asp unit in the hydrophobic Ala-domain (E_{1h}) is significantly higher than in water (E_{1w}). To a very crude approximation ΔE is inversely proportional to the dielectric constant ε of the surrounding medium, so

$$\frac{\Delta E_h}{\Delta E_w} \approx \frac{\varepsilon_w}{\varepsilon_h} \tag{5}$$

where $\varepsilon_w \approx 80$ and $\varepsilon_h \sim 4$ are dielectric constants of water and of hydrophobic bulk Ala region, respectively. While this relation is far from being precise (mainly because it is the *local* dielectric constant ε_{loc} rather than macroscopic ε that is relevant; in the case of water ε_{loc} is much lower than ε), it still shows that $\Delta E_h > \Delta E_w$.

The statistical weight w_0 of a neutral (protonated) Asp unit is

$$w_0 = w_1 e^{\Delta E} c_p v_{bond}$$

where w_1 is the statistical weight of the charged (dissociated) Asp state

$$c_p = 10^{-\text{pH}} \frac{\text{mol}}{\text{L}}$$

is the concentration of protons (H^+), and v_{bond} is the effective volume available for H^+ in the associated state in $COO^- H^+$ group. (k_BT is considered as the energy unit in this section.) The fraction of charged Asp units is

$$\alpha = \frac{w_1}{w_0 + w_1} = \frac{1}{1+\lambda}$$

where $\lambda = w_0/w_1 = v_{bond} c_p e^{\Delta E}$. The parameter λ is related to the pK of the carboxylic group defining the reaction constant for its deprotonation:

$$\lambda = 10^{-\text{pH}+\text{p}K} \tag{6}$$

Hence

$$\text{p}K = \frac{1}{\ln 10}[\Delta E + \ln (v_{bond}[\text{M}]) \tag{7}$$

where

$$[\text{M}] = \frac{\text{mol}}{\text{L}} = N_\text{A}/(10^3\ \text{cm}^3)$$

The pK for Asp in water is[27]

$$\text{p}K = \text{p}K_w \approx 4 \tag{8}$$

pK is slightly higher for Asp at the water/Ala interface (see below) and it is much higher for Asp in Ala domains. In fact, assuming that $v_{bond} \sim 1$ Å^3 (the precise value of v_{bond} is not important), we get from eqs 7 and 8 that $\Delta E_w \approx 17 k_BT$. Formally applying eq 5 leads to $\Delta E_h \sim 340 k_BT$ and $\text{p}K_h \approx 140$ in Ala environment. While thus obtained pK_h is strongly overestimated (for the reason indicated below eq 5), it clearly shows that Asp units located inside the Ala core must be practically neutral. (This conclusion is supported by high experimental pK, p$K \gtrsim 10$, for Asp in nonpolar environment[28]).

Let us now estimate the difference between pK at the Ala/water interface and pK_w. We assume that COO^- subgroup of Asp is exposed to water at the distance h from the Ala/water interface. The dielectric constant of Ala (~4) is much smaller than that of water (≈80). Hence there is a repulsive interaction of COO^- with the interface which is nearly equivalent to the interaction with its mirror-image charge. The corresponding energy is $\Delta\varepsilon \approx {}^1/_4(l_B/h)$, where $l_B = e^2/(\varepsilon_w k_\text{B} T) \approx 7$ Å is the Bjerrum length. For $h \approx 4$ Å (the typical length of Asp monomer) we get $\Delta\varepsilon \approx 0.5$, hence $\text{p}K - \text{p}K_w = \Delta\varepsilon/\ln 10 \approx 0.2$, i.e. $\text{p}K = \text{p}K_i \approx 4.2$ at the interface.

An Asp unit is polar and hydrophilic even in the neutral state: its statistical weight (activity) at the interface with water, w_{0i}, is larger than its activity w_{0h} inside Ala domain: $w_{0h} = e^{-\varepsilon'_P} w_{0i}$, where the free energy difference $\varepsilon'_P \gtrsim 1$ (in k_BT units). On taking into account also the favorable charged state of Asp at the interface we get an even higher total activity there ($\lambda_i \equiv w_{0i}/w_{1i}$): $w_i = w_{0i} + w_{1i} = w_{0i}(1 + 1/\lambda_i) = w_{0i}(1 + 10^{\text{pH}-\text{p}K_i})$. The free energy change on deprotonation (charging) of an Asp-unit at the surface is

$$\Delta\mu_i = -\ln(1+1/\lambda_i) = -\ln(1+10^{\text{pH}-\text{p}K_i}) \tag{9}$$

This decrement is large for high pH (pH above pK_i). The strong preference for the charged state simultaneously means a strong affinity of an Asp unit to the surface. Hence, it seems that nearly all Asp units must be charged and located at the surface of a peptide aggregate at high pH. We return to these statements and analyze their validity in the next section.

4. The Interaction Energy

Let us consider a plane interface between aggregated peptides and water. The energy f_{int} (see eq 3) is associated with interactions of Asp units and counterions at the surface. It consists of several contributions:

$$f_{int} = f_{dis} + f_{ch} + f_{st} \tag{10}$$

Here

$$f_{dis} = \sigma[\alpha \ln \alpha + (1-\alpha)\ln(1-\alpha) + \alpha \ln \lambda_i] \quad (11)$$

is the free energy change on deprotonation of a fraction α of Asp units at the surface (σ is surface concentration of Asp units). f_{ch} accounts for electrostatic interactions of charged Asp units and counterions, and f_{st} is the free energy of nonelectrostatic (excluded-volume) interactions of Asp units at the surface.

At the end of the previous section we argued that the surface Asp units must be fully charged ($\alpha \simeq 1$) at high pH > pK_i. In this case the probability that Asp units are in the interior of the micelle is very low, so we can assume that nearly all Asp units are located at the micelle surface. Although an analysis shows that these assumptions are not always true (see sections 4.2 and 4.3), it is instructive to first adopt the condition $\alpha \simeq 1$ and then to consider its consistency. This is done below.

4.1. Electrostatic Surface Energy: Fully Charged Asp. Let us calculate the electrostatic energy f_{ch} for a flat peptide/water interface with a known surface concentration of Asp units, σ. The interface can be approximated by a uniformly charged surface ($x = 0$, where x is the coordinate normal to the surface) with surface charge density $\zeta = -e\sigma\alpha \simeq -e\sigma$ since $\alpha \simeq 1$. The surface is separating the peptide phase ($x < 0$) and water ($x > 0$). There are no charges inside the peptide (Ala) phase, hence electric field $= 0$ there. The electric field in the other half-space ($x > 0$) is screened by ions dissolved in water; the ionic strength in the bulk of water is I_∞ (for example, $I_\infty = 10^{-\mathrm{pH}}$[M] in the case of no salt and pH < 7). The ion distribution in water is predicted by the classical mean-field theory (the Gouy−Chapman theory[25]). The relevant Poisson−Boltzmann (PB) equation is

$$\frac{d^2\Phi}{dx^2} = 4\pi l_B \varrho \quad (12)$$

where $\Phi = -e\varphi/(k_BT)$ is the reduced electric potential ($\varphi = \varphi(x)$ is the local electric potential), $\varrho = I_\infty(e^{\Phi} - e^{-\Phi})$ is the reduced density of charge in the diffuse ion layer (all ions are assumed to be monovalent), and

$$l_B = \frac{e^2}{\varepsilon_w k_B T}$$

The boundary condition is

$$\frac{d\Phi}{dx} = 4\pi\varepsilon \frac{e}{\varepsilon_w k_B T} \simeq -4\pi l_B \sigma \quad \text{at } x = +0 \quad (13)$$

The solution to the PB eq 12

$$\Phi(x) = 2\ln\frac{1+\beta e^{-x/r_D}}{1-\beta e^{-x/r_D}} \quad (14)$$

where r_D is the Debye length ($r_D^{-2} = 8\pi l_B I_\infty$), and β is defined by the boundary condition (the approximation sign "≃" is replaced by "=" here):

$$\frac{2\beta}{1-\beta^2} = \Lambda, \quad \Lambda \equiv 2\pi l_B r_D \sigma = \frac{r_D}{h_{GC}} \quad (15)$$

Here h_{GC} is the characteristic thickness of the diffuse ion layer (the Gouy−Chapman length):

$$h_{GC} = \frac{1}{2\pi l_B \sigma} \quad (16)$$

The electrostatic interaction free energy (per unit area) is

$$f_{ch}/k_BT = \int \Phi(0)\, d\sigma = 2\sigma\left\{\ln\frac{1+\beta}{1-\beta} - \beta\right\}$$

Using eq 15 we get in the regime $\Lambda \gg 1$ (i.e., $h_{GC} \ll r_D$)

$$f_{ch} \simeq 2\sigma \ln\frac{4\pi l_B r_D \sigma}{e} \quad (17)$$

Next we note that f_{dis}, eq 11, simplifies for $\alpha \simeq 1$ as

$$f_{dis} \simeq \sigma\Delta\mu_i$$

where $\Delta\mu_i$ is defined in eq 9.

Using eqs 1, 2, 3, 10, 17 we obtain the free energy per peptide in a micellar structure $\Delta F = F - F_{core}$ (in k_BT units):

$$\Delta F = F_s + F_{loc} \approx A\left[\frac{\gamma_0}{k_BT} + \sigma\Delta\mu_i + 2\sigma\ln\frac{4\pi l_B r_D\sigma}{e} + f_{st}\right] + n_{Pb}\ln\frac{V^*}{A\Delta} \quad (18)$$

where $\Delta \sim 0.4$ nm is the interfacial layer thickness. Note that the energy F_{core} is irrelevant here as it does not depend on σ. Taking into account that $A = n_P/\sigma$ (since all Asp units are assumed to be at the surface), neglecting the excluded-volume term f_{st} (the steric repulsion of Asp), and minimizing F with respect to σ we find the optimum surface concentration (note that the parameters γ_0, $\Delta\mu_i$, V^*, Δ are independent of σ)

$$\sigma = \sigma^* \simeq \frac{\gamma_0}{k_BT}\frac{1}{2 + n_{Pb}/n_P} \quad (19)$$

The poly-alanine/water interfacial tension is $\gamma_0 \approx 45$ dyn/cm,[24] yielding $\sigma^* \approx 3.7$ nm^{-2} for peptides P1, P4 ($n_P/n_{Pb} = 1$) and $\sigma^* \approx 4.4$ nm^{-2} for peptides P2, P3 ($n_P/n_{Pb} = 2$). The obtained densities σ are high: in fact, they are higher than the maximum density σ_{max} in a monolayer of close-packed Asp-units.[17] Hence, the f_{st} term cannot be neglected. The precise dependence $f_{st}(\sigma)$ is not known (and is not universal); however, a reasonable approximation can be provided by the lattice−gas theory:

$$f_{st}(\sigma) \approx (\sigma_{\max} - \sigma)\ln\left(1 - \frac{\sigma}{\sigma_{\max}}\right) \quad (20)$$

(A similar expression accounts for the excluded-volume interaction in polymer mixtures in the framework of the classical Flory−Huggins theory.[29])

Minimization of ΔF including f_{st}, eq 20, shows that the latter term essentially leads to a reduction of σ^* down to a value slightly below σ_{max} for P1, P3 and P4 peptides, i.e.

$$\sigma^* \sim \sigma_{\max} \approx 3\ \mathrm{nm}^{-2} \quad (21)$$

The corresponding Gouy−Chapman length is

$$h_{GC} = \frac{1}{2\pi l_B \sigma^*} \sim 0.075\ \mathrm{nm} \quad (22)$$

The predicted electrical double layer of counterions is thus very thin ($\Lambda \gg 1$). The layer thickness is much smaller than both r_D and the radius of curvature of the interface (which is

of the order or longer than the peptide contour length $L = nl_1$, $n = n_H + n_P$). Hence the surface curvature effects are likely to be small.

We are now in a position to estimate the main surface contributions to the free energy F per peptide for the optimal $\sigma = \sigma^*$. The γ_0-term in eq 18 amounts to

$$\frac{n_P}{\sigma^*}\gamma_0 \sim 7.5(k_B T)$$

while the electrostatic term is

$$2n_P \ln\frac{4\pi l_B r_D \sigma}{e} \gtrsim 9(k_B T)$$

for $r_D \gtrsim 1$ nm. Both energies are therefore much larger than the conformational (elastic) energy of a peptide molecule, $\Delta F_{el} \lesssim k_B T$ (see the end of section 2.2).

The results considered above imply that concentration of counterions near the surface ($x = 0$) is high. This leads to the following problem if all the cations are protons (which is the case for pH < 7, no added salt): a high concentration of protons near the surface (corresponding to a low *local* $\mathrm{pH}|_{x=0} = \mathrm{pH}_i$) means that most Asp units at the surface can be neutralized (protonated) if $\mathrm{pH}_i < \mathrm{p}K_i$. The assumption $\alpha \simeq 1$ must be lifted in this regime as considered in the next section.

4.2. pH < 7, No Salt. Let us consider the regime when there are no other cations in the water phase except protons, i.e. pH < 7, no salt. In the presence of electric potential φ the concentration of protons increases to $c_p = 10^{-\mathrm{pH}} e^{\Phi}$[M], where $\Phi = -e\varphi/(k_B T)$, e is the proton charge. The degree of charge of Asp units at the surface, α, changes as a result:

$$\alpha = \frac{1}{1 + \lambda e^{\Phi(0)}} \tag{23}$$

where $\lambda = 10^{\mathrm{p}K_i - \mathrm{pH}}$. α gets lower for $\Phi(0) > 0$ leading to a lower surface charge density $\zeta = -e\sigma\alpha$. In this case σ must be replaced by $\sigma\alpha$ in eqs 13, 15, 16. Equation 14 stays valid, hence

$$\Phi(0) = 2\ln\frac{1+\beta}{1-\beta} \tag{24}$$

where β is defined by

$$\frac{2\beta}{1-\beta^2} = \Lambda\alpha, \quad \Lambda = 2\pi l_B r_D \sigma \tag{25}$$

In the previous section, we showed that $\Lambda \gg 1$. Equations 23, 24, and 25 can now be solved for β and α. In the most interesting regime, $\Lambda\alpha \gg 1$, we get the following equation for α:

$$\alpha = \frac{1}{1 + 4\lambda\Lambda^2\alpha^2} \tag{26}$$

The parameter $4\lambda\Lambda^2 = 2\pi\sigma^2 10^{\mathrm{p}K_i} l_B/[\mathrm{M}]$ is very large ($\sim 10^6$) for $\sigma \sim \sigma_{max}$ (note that $r_D^{-2} = 8\pi l_B I_\infty$, and $I_\infty = 10^{-\mathrm{pH}}$[M]). Therefore, to a good approximation

$$\alpha \simeq (4\lambda\Lambda^2)^{-1/3} = (2\pi\sigma^2 10^{\mathrm{p}K_i} l_B/[\mathrm{M}])^{-1/3} \tag{27}$$

It is remarkable that the fraction of charged Asp units is independent of pH in this regime. Using the last equation we get $\alpha \sim 10^{-2}$ for $\sigma \sim \sigma_{max}$, i.e. the Asp units are just very weakly charged at the surface (only about 1%, or less, of Asp units are charged). This also leads to a lower affinity of Asp units to the surface (as most of these units are neutral). Such low fraction of charged Asp units is very unlikely to induce a significant reduction of the surface tension required for micelle stabilization (see sections 5.2 and 5.3).

4.3. The Effect of Salt. A high degree of charge (α close to 1) is generally necessary for micelle stability (see section 5.3). Clearly, this regime is accessible only if there are a lot of cations other than protons in the water phase, i.e. if either a sufficient amount of salt is added or pH is significantly higher than 7. Accordingly, below we consider the regime of relatively high ionic strength: $I_\infty \gg c_p = 10^{-\mathrm{pH}}$[M] (this is in contrast to the previous section where $I_\infty = c_p$). In this case it is necessary to take into account that added cations have finite size ($\sim \delta$), so that there is a dead layer near the charged surface ($0 < x < \delta$) which is inaccessible for the cations (the charge due to protons in this layer can be neglected since their concentration must be low there to avoid neutralization of Asp units). Such a δ-layer was introduced long ago in the Stern generalization[30] of the Gouy−Chapman model.[25] The solution to the PB equation then modifies as

$$\Phi(x) = \begin{cases} 4\pi l_B \sigma\alpha(\delta - x) + 2\ln\dfrac{1+\beta}{1-\beta}, & x < \delta \\ 2\ln\dfrac{1+\beta e^{-(x-\delta)/r_D}}{1-\beta e^{-(x-\delta)/r_D}}, & x > \delta \end{cases}$$

where β is still defined in eq 25. In particular

$$\Phi(0) = 4\pi l_B \sigma\alpha\delta + 2\ln\frac{1+\beta}{1-\beta} \tag{28}$$

Assuming $\Lambda\alpha \gg 1$ as before, we get instead of eq 26:

$$\alpha = \frac{1}{1 + 4\lambda\Lambda^2 e^{\nu\alpha}\alpha^2} \tag{29}$$

where $\nu = 4\pi l_B \sigma\delta$. The solution for α is $\alpha \simeq 1$ if

$$4\lambda\Lambda^2 e^{\nu} \ll 1$$

i.e.

$$I_\infty \gg 2\pi e^{4\pi\sigma l_B \delta} l_B \sigma^2 10^{\mathrm{p}K_i - \mathrm{pH}} \tag{30}$$

The latter condition (defining the strong charge regime) is satisfied if ionic strength and/or pH is high enough. For example, $\alpha \sim 1$ for $I_\infty \gtrsim 0.1$ [M] if $\delta = 3$ Å, $\sigma = 2$ nm^{-2}, and pH = 9.

In order to obtain the total electrostatic free energy $f = f_{ch} + f_{dis}$ we use the theorem on small variations[31] saying that

$$\frac{\partial f}{\partial \varepsilon} = \sigma\alpha$$

where ε is the deprotonation energy associated with pK ($e^{\varepsilon} = 10^{\mathrm{p}K}$). Obviously $f = 0$ for $\varepsilon = \infty$ (neutral system), hence

$$f = -\sigma\int_{\varepsilon}^{\infty} \alpha\, d\varepsilon \tag{31}$$

Evaluating the integral in the strong charge regime ($\alpha \simeq 1$ for the actual ε) we get:

$$f/\sigma \simeq \ln 10(\mathrm{p}K - \mathrm{pH}) + 2\ln\frac{4\pi l_B \sigma r_D}{e} + \nu/2$$

hence

$$f_{ch}/\sigma \simeq 2\ln\frac{4\pi l_B \sigma r_D}{e} + 2\pi l_B \sigma \delta \tag{32}$$

For point-like cations ($\delta = 0$), the last equation coincides with eq 17.

The total free energy per peptide molecule $\Delta F = F - F_{core}$ in the strong charge regime, $\alpha \simeq 1$, is (in k_BT energy units)

$$\Delta F = F_s + F_{loc} \simeq n_P\left[\frac{\gamma_0}{\sigma} + \ln 10\ (\mathrm{p}K_i - \mathrm{pH}) + 2\ln\frac{4\pi l_B \sigma r_D}{e} + 2\pi l_B \sigma\delta + \frac{f_{st}}{\sigma}\right] + n_{Pb}\ln\left(\frac{\sigma V^*}{n_P \Delta}\right) \tag{33}$$

The optimum surface concentration σ^* of Asp units can be obtained by minimizing F with respect to σ. Neglecting the steric term f_{st} we find:

$$\sigma^* \approx \frac{2\gamma_0}{s + \sqrt{s^2 + 8\pi l_B \delta \gamma_0}} \tag{34}$$

where $s \equiv 2 + n_{Pb}/n_P$. In particular, the last equation gives

$$\sigma^*/\sigma_{\max} \approx 0.65 \text{ for } \delta = 3\text{ Å}, \quad \approx 0.55 \text{ for } \delta = 5\text{Å}$$

with $\gamma_0 \approx 45$ dyn/cm, $n_{Pb} = n_P$ (P1 and P4 peptides). Taking into account the steric term (using eq 20) we find that its effect is to slightly reduce, by 6% and 4%, respectively, the above values of σ^*.

5. Equilibrium Results

5.1. Micellar Shape. Let us consider a dilute peptide solution in the high salt regime where micelle formation is expected (the critical micelle concentration is discussed below in section 5.2) and where nearly all peptidic Asp groups are located at the micelle surface and are charged ($\alpha \simeq 1$, the strong charge regime). What are the main factors defining the micelle morphology in this regime? It turns out that the micellar shape is largely determined by simple geometrical parameters: the optimum volume of the hydrophobic (H) core V^*, the optimum interfacial area A^* and the maximum distance R from a point in an H-domain to the nearest interfacial point (for example, R is just the radius for a spherical or a cylindrical micelle; in the case of peptide bilayer R is half-thickness of the layer). The optimum area per peptide, $A^* = n_P/\sigma^*$, can be treated as a constant since the curvature effects are negligible in the first approximation: while bending energy F_{bend} is significant for high interfacial curvature $C \sim C^* \sim 1/\Delta$, F_{bend} provides just a small correction to F_s for micellar structures characterized by either $C = 0$ (for plane layers) or $C \sim 1/R \ll C^*$ (for nonplanar structures with the characteristic micelle size $R \sim L = nl_1 \gg \Delta$).

The crucial nondimensional parameter is the reduced area $\theta = A^*R/V^*$. A simple geometrical consideration shows that $\theta = 3$ for spheres, $\theta = 2$ for cylinders, and $\theta = 1$ for planar layers. (Inverse micellar structures of solvent microdomains in the peptide precipitate are not considered here for simplicity.) Let us estimate θ based on the peptide molecular structure. Since all Asp (P) units are at the surface, and Ala (H) units are in the core, some hydrophobic fragments have to span the distance R from the surface to the core "center". Therefore, R cannot exceed the maximum contour length L_{max} between an H-unit and the nearest (along the chain) P-unit. It is obvious that $L_{max} = L/n_j$, where $n_j = 2, 1, 2$, and 2 for P1, P2, P3, and P4 peptides, respectively ($L = nl_1$ is the peptide contour length). A simple analysis shows that the geometrical and packing restrictions (namely, the conditions that all H-units are uniformly distributed in the core respecting chain connectivity, while all P-units are at the surface) do allow formation of micellar structures of any of the 3 shapes (spherical, cylindrical, plane layer) with almost any R below L_{max} for any of the 4 peptides with only one exception: The plane membrane structure of P4-peptides with half-width $R > {}^2/_3 L_{\max}$ is not possible. The reason is that although the second H-block of P4 (with free H-end) can be extended to L_{max}, the first blocks (terminated by P-units) must form loops giving rise to tripling of H-density in the core layers adjacent to the surface as compared to the central core layer. A homogeneous core is possible only for $R < R_{max} = L/3$. Thus

$$R_{\max}/L = \begin{cases} 1/3 & \text{for P4, layers} \\ 1/n_j & \text{in all other cases} \end{cases}$$

The important parameter is

$$\theta_{\max} = \frac{A^* R_{\max}}{V^*} = \frac{n_P}{\sigma^* A_1}\frac{R_{\max}}{L}$$

where

$$A_1 = \frac{V^*}{L} \approx \frac{M_{1H}}{\rho_0 N_A l_1} \approx 0.25\ \mathrm{nm}^2$$

is the effective cross-section of the peptide chain. Note that $1/\theta_{max}$ is distinct from, but is akin to the classical surfactant packing parameter[32] (one difference is that R_{max} is not simply the molecular length).

If $\theta_{max} > 3$, then optimum micelles (with $\sigma = \sigma^*$) of any geometry (spherical, cylindrical or plane layer) are possible. The main contributions to the free energy per molecule (namely, the core contribution and the surface energy F_s) are the same for all three structures. However, the curvature is more favorable for spherical micelle. Indeed, the bending energy, eq 4, is dominated by the first linear term

$$F_{bend} \simeq -\kappa CA = -\kappa C n_P/\sigma^*$$

where C is the mean curvature and $\kappa > 0$ (convex interface is favorable). Now, $C = 2/R = 2A/(3V)$ for spherical micelle, $C = 1/R = A/(2V)$ for cylindrical micelle, and $C = 0$ for layers. Therefore, the spheres are characterized by the most favorable bending energy, while the layers are least favorable. Hence, it is the spheres that are predicted for $\theta_{max} > 3$. For a similar reason the cylinders are favorable if $2 < \theta_{max} < 3$, and the plane membranes if $1 < \theta_{max} < 2$. A structure with the optimum surface concentration of P-units (i.e., with $\sigma = \sigma^*$) is not allowed for $\theta_{max} < 1$: in this case the membranes with $\sigma = \theta_{max}\sigma^*$, $\sigma < \sigma^*$, are favored.

Thus, for P1, P3, and P4 peptides the spherical micelles are predicted for $\sigma^* A_1 < {}^1/_3$, cylinders for ${}^1/_2 < \sigma^* A_1 < {}^1/_3$, and plane membranes for $\sigma^* A_1 > {}^1/_2$. The critical values of $\sigma^* A_1$ (${}^1/_3$, ${}^1/_2$) change to (${}^2/_3$, 1) for the P2 peptide.[18] The phase diagrams in variables γ_0, δ obtained using eq 34 for the four peptides are shown in Figure 2.

Compact spherical micelles of radius

$$R \approx \frac{3\sigma^* A_1}{n_P} L$$

are formed if either the cation size δ is large enough, and/or if the reference Ala/water surface tension γ_0 is low enough (see the regions above the solid lines marked Pi, $i = 1, 2, 3, 4$, in Figure 2). In other words, the equilibrium may be shifted

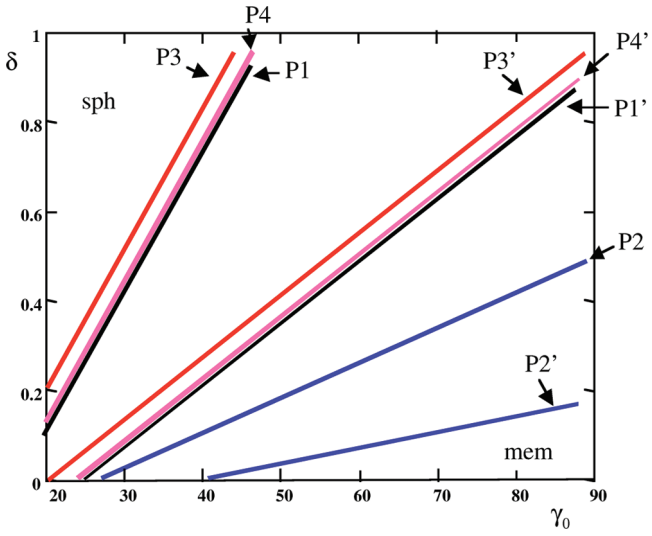

Figure 2. Phase diagrams for the peptides P1−P4 in variables: γ_0 (the reference surface energy at the interface between hydrophobic units and water, in dyn/cm) vs δ (the characteristic cation size, in nm). For a solution of P*i*-peptides (i = 1,2,3,4), spherical aggregates are predicted above the solid line marked as P*i*; the region of cylindrical filaments is between the lines marked as P*i* and P*i*′; membranes are predicted below the P*i*′-line.

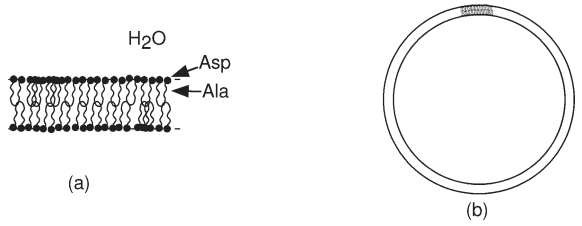

Figure 3. (a) Plane bilayer membrane of P1-peptides. (b) Closed membrane forming a vesicle.

from layers (membranes; see Figure 3) to cylindrical and spherical micelles by decreasing γ_0, i.e. by decreasing hydrophobicity of Ala fragments. The number of peptides in a spherical micelle is

$$Q \approx \frac{4\pi R^3}{3V^*}$$

so the aggregation number for $Ala_{24}Asp_2$ peptides amounts to $Q \approx 500$ for $\delta = 3$ Å. Plane membranes (or vesicles), Figure 3, are formed in the opposite regime of small δ, high γ_0 (below the lines marked as P*i*′). The membrane thickness is

$$H \approx \frac{2\sigma^* A_1}{n_P} L$$

Long cylindrical aggregates are predicted in the intermediate regime between the P*i* and P*i*′ lines; the cylinder radius is

$$R \approx \frac{2\sigma^* A_1}{n_P} L$$

Generally, the P2-peptides have the strongest tendency to form spherical micelles, and the P3-peptides rather tend to form membranes or cylinders, while the P1 and P4 peptides show an intermediate behavior. For example, for $\delta = 3$ Å and $\gamma_0 \approx 45$ dyn/cm, it is predicted that P2-peptides self-assemble in spheres of radius $R \approx 2.8$ nm, P3-peptides form layers of thickness $H \approx 1.9$ nm, and P1 and P4 peptides are close to the boundary between membrane and filament morphologies in the same conditions.

5.2. Critical Micelle Concentration. Generally, the micelles are formed if the peptide volume fraction ϕ exceeds the so-called critical micelle concentration (CMC) ϕ_C: $\phi > \phi_C$. The latter is roughly defined by the following equation:

$$\ln\phi_C \approx F_{mic} - F_{dis} \tag{35}$$

where $F_{mic} - F_{dis}$ is the excess free energy per peptide molecule in a micelle as compared with dissolved peptides.

$$F_{mic} \approx F_{core} + \Delta F \tag{36}$$

where $F_{core} = -n_H\varepsilon_H$, and ΔF is defined in eq 33 with σ defined in eq 34. The strong charge regime ($\alpha \simeq 1$, see eq 30) is considered here since micelles are hardly formed otherwise. (The steric term $F_{st} = f_{st}n_P/\sigma$ in eq 33 is neglected in what follows for the reasons outlined below eq 34.) The case of monovalent ions is assumed as before. Note that eq 36 is applicable whatever is the micelle geometry: the free energy difference related to the micellar shape is small and is neglected here.

The free energy in the dissolved state is

$$F_{dis} = n_P(-\varepsilon_P + \Delta\mu)$$

where ε_P is the free energy gained when a *neutral* P-unit is transferred from micelle interface to the bulk water, and $\Delta\mu$ accounts for the effect of ionization of a P-unit in water. $\Delta\mu$ in water can be found in analogy with eq 9:

$$\Delta\mu = -\ln(1 + 10^{\mathrm{pH} - \mathrm{p}K_w}) \simeq \ln 10\ (\mathrm{p}K_w - \mathrm{pH})$$

The micelles are formed at all if $F_{mic} < F_{dis}$. Using equations above we get

$$\ln\phi_C \approx \mathrm{const} + 2n_P \ln r_D + n_P\left[\frac{\gamma_0}{\sigma} + 2\ln\sigma + 2\pi l_B\delta\sigma\right] + n_{Pb}\ln\frac{V^*\sigma}{n_P\Delta} \tag{37}$$

where $\mathrm{const} = -n_H\varepsilon_H + n_P\varepsilon_P + n_P \ln 10\ (\mathrm{p}K_i - \mathrm{p}K_w) + 2n_P \ln(4\pi l_B/e)$ (all the parameters involved in const are treated as fixed). It is not our aim to quantitatively predict CMC for $Ala_{24}Asp_2$ peptides. This is not possible since CMC strongly (exponentially) depends on unknown parameters like ε_H and ε_P. It is clear that CMC exponentially decreases with the length of hydrophobic part, n_H, so it can be made however small. Below we discuss qualitatively, based on eq 37, how CMC depends on the main solution parameters (pH, ionic strength I_∞, cation size δ), on the surface tension γ_0 and on the peptide structure.

CMC, as defined in eq 37, does not depend on pH. This feature is true in the strong charge regime ($\alpha \simeq 1$). More precisely, CMC starts to decrease as pH drops down to the regime where $\alpha \sim 0.5$, i.e. where the strong charge condition 30 ceases to be valid and micelles get readily destabilized with respect to precipitation. The CMC decrease is moderate unless n_P is large.

Let us turn to the dependence of CMC on other parameters. CMC always decreases with I_∞ as

$$\phi_C \propto I_\infty^{-n_P} \tag{38}$$

CMC increases with δ, and it also formally increases with γ_0, i.e., with the degree of hydrophobicity of Ala units (formally,

since the effect of γ_0 increase is likely to be masked by the parallel increase of ε_H leading to lower CMC). For low $\gamma_0\delta$

$$\phi_C \propto \gamma_0^{2n_P+n_{Pb}}, \quad \gamma_0\delta \ll 1/(2\pi l_B) \tag{39}$$

so ϕ_C just slightly depends on δ in this regime. For high $\gamma_0\delta$, the CMC dependence on both parameters is strong:

$$\phi_C \propto e^{n_P\sqrt{8\pi l_B\delta\gamma_0}}, \quad \gamma_0\delta \gg 1/(2\pi l_B) \tag{40}$$

Turning to the CMC dependence on the peptide structure: It is clear that CMC is significantly lower for P2 and P3 peptides than for P1 and P4 peptides due to a lower Asp-localization free energy (lower n_{Pb}) for the former pair. In addition, we expect a slightly lower CMC for P2 than for P3 peptide. This difference (which is not reflected in eq 37) is due to the effect of steric free energy F_{st} neglected before: In the case of P2 the Asp-Asp dimer at the chain end can be oriented perpendicular to the interface thus reducing the "excluded area" per Asp unit. Such dimer conformation is not likely for P3: in this case the dimer is expected to be oriented parallel to the interface due to the presence of two Ala-tails. As for the pair P1, P4, we expect a slightly lower CMC for P4 peptide due to a bit smaller Asp-localization energy contribution: the two Asp units are connected by a shorter bridge in the case of P4, hence once one Asp unit is localized at the surface, the other is less free (more confined by the connecting bridge) in the case of P4 than for P1 peptide (this effect is not captured in eq 37).

5.3. Precipitation vs Micellization. Formation of micelles may be suppressed due to peptide precipitation (macroscopic phase separation). Micelles are favorable only if their free energy F_{mic} is lower than the free energy of the precipitate F_{pr}, $F_{mic} < F_{pr}$. Assuming the homogeneous precipitate, we write

$$F_{pr} = -\varepsilon_H n_H + \varepsilon_P' n_P \tag{41}$$

where ε'_P is the free energy required in order to transfer an uncharged Asp unit from Ala/water interface to the interior of the precipitate (the sum $\varepsilon'_P + \varepsilon_P$ is thus the free energy increase when one neutral Asp unit is transferred from water phase to the precipitated peptide phase; note that Asp units in the Ala environment are always neutral, see section 3.1).

In the strong charge regime (see eq 30) the condition $F_{mic} < F_{pr}$ reads:

$$n_P\left[\frac{\gamma_0}{\sigma} + \ln 10\ (\mathrm{p}K_i - \mathrm{pH}) + 2\ln\frac{4\pi l_B\sigma r_D}{e} + 2\pi l_B\sigma\delta\right] + n_{Pb}\ln\left(\frac{\sigma V^*}{n_P\Delta}\right) < \varepsilon_P' n_P \tag{42}$$

The approximations involved in this expression are outlined at the beginning of section 5.2. Using the condition 42, we find that micelles are stable if $I_\infty 10^{\mathrm{pH}}$ is high enough:

$$I_\infty 10^{\mathrm{pH}} > \Pi_m \tag{43}$$

where

$$\Pi_m \approx 2\pi l_B\sigma^2 10^{\mathrm{p}K_i} e^{4\pi l_B\delta\sigma}\left(\frac{V^*\sigma e}{n_P\Delta}\right)^{n_{Pb}/n_P} e^{-\varepsilon_P'} \tag{44}$$

(for $\sigma = \sigma^*$). The threshold Π_m increases with $\mathrm{p}K_i$, δ, n_{Pb}, γ_0 (since larger γ_0 leads to higher $\sigma = \sigma^*$), and it decreases with ε'_P. Π_m is higher (less stable micelles) for P1, P4 peptides than for P2, P3. As an example we get:

$$\Pi_m \approx 0.8 \times 10^8\,[\mathrm{M}]$$

for $\varepsilon'_P = 1$ (k_BT), $n_{Pb}/n_P = 0.5$ (for P2, P3 peptides), $\gamma_0 \approx 45$ dyn/cm (i.e., $\gamma_0 \approx 11 k_BT/\mathrm{nm}^2$), $\delta = 3$ Å, $\Delta = 4$ Å, and $\sigma = \sigma^*$. Therefore, in this case micelles can be stable, for example, in the region pH > 10 and $I_\infty > 0.01$[M]. A slightly higher threshold, $\Pi_m \approx 1.2 \times 10^8$[M], is obtained for $n_{Pb}/n_P = 1$ (for P1, P4 peptides) with otherwise the same parameters.

Equation 44 somewhat simplifies for $\gamma_0\delta \ll 1/(2\pi l_B)$:

$$\Pi_m \simeq 2\pi l_B 10^{\mathrm{p}K_i} e^{s-\varepsilon_P'-2}\left(\frac{\gamma_0}{s}\right)^s\left(\frac{V^*}{n_P\Delta}\right)^{s-2}$$

where $s = 2 + n_{Pb}/n_P$. In the opposite regime, $\gamma_0\delta \gg 1/(2\pi l_B)$, we get:

$$\Pi_m \simeq 2\pi l_B 10^{\mathrm{p}K_i}\left(\frac{\gamma_0}{2\pi l_B\delta}\right)^{s/2} e^{\sqrt{8\pi l_B\delta\gamma_0}}\left(\frac{V^*}{n_P\Delta}\right)^{s-2} e^{s-2-\varepsilon_P'}$$

Obviously, Π_m strongly increases with both δ and γ_0 in this regime.

The general condition of micelle stability, eqs 43 and 44, are rather similar to the strong charge condition, eq 30: the latter can be rewritten as $I_\infty 10^{\mathrm{pH}} \gg \Pi_{sc}$, where

$$\Pi_{sc} = \Pi_m\left(\frac{V^*\sigma e}{n_P\Delta}\right)^{-n_{Pb}/n_P} e^{\varepsilon_P'}$$

The difference between Π_{sc} and Π_m is not great. For example, for $\varepsilon'_P = 1$ (k_BT), $n_{Pb}/n_P = 0.5$ (P2, P3 peptides), $\gamma_0 \approx 45$ dyn/cm, $\delta = 3$ Å, $\Delta = 4$ Å, we get: $\Pi_{sc} \approx \Pi_m$. Therefore, as a rule of thumb, micelles get destabilized as soon as the degree of charge of their surface Asp units drops to a moderate level $\alpha \sim 1/2$. Micelles with weakly charged Asp units can remain stable if $\varepsilon'_P \gg k_BT$ which is however rather unlikely since neutral Asp (P) units are not expected to be strongly hydrophilic (recall that ε'_P is the difference between the chemical potentials of a *neutral* Asp unit in the Ala environment and at the Ala/water interface).

Indefinite aggregation of peptides (rather than micelle formation) becomes favorable in the regime where the condition 43 is violated. Formation of large aggregates (peptide droplets that grow in size) is expected in this regime. The driving force for the growth of peptide aggregates is the positive *effective* surface tension γ_0^* (the free energy increment corresponding to a unit area increase of the total surface area). The renormalization of γ_0 is due to the effect of Asp units: although most of Asp units have to be located inside a large peptide aggregate (since the aggregate's size R is larger than the peptide length L), still some Asp units can reach the surface and stay there in the favorable charged state. The tension γ_0^* can be easily obtained:

$$\gamma_0^* \simeq \gamma_0 - \sigma\varepsilon_P' + f_{int} + \frac{n_{Pb}}{n_P}\ln\left(\frac{V^*\sigma}{n_P\Delta}\right) \tag{45}$$

where the last term reperesents the localization free energy, $f_{int} = f + f_{st}$, and f is defined in eq 31. The equilibrium effective tension $\gamma = \gamma_0^*$ corresponds to the minimum of γ_0^*

with respect to σ:

$$\gamma = \min_{\sigma} \gamma_0^* \quad (46)$$

It is easy to show that the condition $\gamma < 0$ is equivalent to the condition of micelle stability, $F_{mic} < F_{pr}$. On the other hand, $\gamma > 0$ in the precipitation regime roughly corresponding to $I_\infty 10^{\mathrm{pH}} < \Pi_m$. (Note that at the threshold $\gamma = 0$ the equilibrium concentration of Asp units at the surface of a large aggregate is $\sigma = \sigma^*$: $\gamma_0^*(\sigma^*) = 0$ for $\gamma = 0$.) The effective tension γ decreases at higher pH or I_∞ (following the variation of f, eq 31, and α, eq 29, with these parameters); γ can be much lower than γ_0 if $I_\infty 10^{\mathrm{pH}}$ is close to the threshold Π_m. On the other hand, $\gamma \approx \gamma_0$ for low enough $I_\infty 10^{\mathrm{pH}}$ when the peptide/water interface is just weakly charged.

The macroscopic peptide phase (the precipitate) is formed in the regime $\gamma > 0$ if $\phi > \phi_{CPC}$, where the critical precipitation concentration (CPC) is defined by (compare with eq 35):

$$\ln \phi_{CPC} \approx F_{pr} - F_{dis}$$

Hence

$$\ln \phi_{CPC} \approx -\varepsilon_H n_H + (\varepsilon_P + \varepsilon_P' + \ln(1 + 10^{\mathrm{pH} - \mathrm{p}K_w}))n_P \quad (47)$$

Note that CPC strongly depends on pH for pH $>$ pK_w:

$$\phi_{CPC} \propto 10^{\mathrm{pH} \cdot n_P}$$

In this regime, CPC decreases by a factor of 100 when pH is decreased by 1 (for $n_P = 2$).

6. Kinetic Stabilization of Finite Aggregates

Let us consider the regime where precipitation is thermodynamically more favorable than micellization (i.e., pH $< \log_{10}(\Pi_m/I_\infty)$). In this regime finite micelles are not stable thermodynamically: they tend to further aggregate. However, micelles can still repel each other in this regime since their surfaces are charged, and this repulsion is rather long-range (it extends to $r_D \gtrsim 1$ nm). Micelle aggregation can be significantly slowed down due to their electrostatic repulsion, i.e. aggregates of finite size can be kinetically stabilized against further fusion. This electrostatic stabilization mechanism is considered below.

The main part of the repulsion energy between two aggregates comes from the interaction between their closest (and nearly parallel) surface parts. Therefore, by virtue of the Derjaguin approximation, the problem can be reduced to the interaction of parallel Gouy−Chapman layers. Below we will focus on the regime

$$h_{GC} \ll r_D \quad (48)$$

where

$$h_{GC} = \frac{1}{2\pi l_B \sigma \alpha}$$

and α is the fraction of charged Asp units at the surface (compare with eq 16). α can be obtained solving eq 29 which, in the weak charge regime ($\alpha \ll 1$), simplifies as

$$\alpha^3 e^{v\alpha} \simeq \frac{I_\infty 10^{\mathrm{pH} - \mathrm{p}K_i}}{2\pi\sigma^2 l_B} \quad (49)$$

The condition 48 is valid (for $\sigma \sim \sigma_{max} \sim 3$ nm^{-2}, see eq 21) if $I_\infty/[\mathrm{M}] \lesssim \alpha^2$, for example, if the ionic strength $I_\infty \sim 10^{-2}$[M] and the degree of surface charge $\alpha \sim 0.1$.

6.1. Interaction of Two Gouy−Chapman Layers. Consider two parallel Gouy−Chapman layers[25] separated by distance d: one layer at $x = 0$ and the other at $x = d$. The reduced electrostatic potential Φ satisfies the PB equation (compare with eq 12):

$$\frac{\mathrm{d}^2\Phi}{\mathrm{d}x^2} = \frac{1}{{r_D}^2}\sinh \Phi$$

with boundary conditions

$$\frac{\mathrm{d}\Phi}{\mathrm{d}x} = \pm 4\pi l_B \sigma \alpha$$

at $x = d, 0$.

The repulsion force per unit area (pressure) τ is proportional to the excess pressure of ions in the middle plane between the layers:

$$\tau = 2I_\infty(\cosh \Phi_m - 1)$$

where $\Phi_m = \Phi(d/2)$. Integrating the PB equation and using the boundary conditions one gets:

$$\frac{d}{2} = 2\int_0^{r_D/h_{GC}} \frac{\mathrm{d}y}{\sqrt{(2y^2 + \cosh \Phi_m)^2 - 1}}$$

This equation implicitly defines Φ_m as a function of d. The upper limit of integration can be set to ∞ for $d \gg h_{GC}$ (since $r_D/h_{GC} \gg 1$). The following asymptotic behaviors of the electrostatic force can be obtained as a result:

$$\tau \simeq \frac{k_B T}{l_B} \begin{cases} \dfrac{\pi}{2d^2}, & h_{GC} \ll d \ll r_D \\ \dfrac{8}{\pi {r_D}^2} \mathrm{e}^{-d/r_D}, & d \gg r_D \end{cases} \quad (50)$$

The corresponding energy of electrostatic interaction per unit area is

$$w(d) \simeq \frac{k_B T}{l_B} \begin{cases} \dfrac{\pi}{2d}, & h_{GC} \ll d \ll r_D \\ \dfrac{8}{\pi r_D} \mathrm{e}^{-d/r_D}, & d \gg r_D \end{cases} \quad (51)$$

The above equations constitute the classical results obtained within the frameworks of Gouy−Chapman[25] and DLVO[33] theories.

6.2. Kinetic Stabilization of Spherical Aggregates. Using the Derjaguin approximation[34] we relate the interaction energy $F(d_0, R)$ of two spherical droplets (of radius R, with the minimum distance d_0 between their surfaces, $d_0 \ll R$) to the interaction of two parallel Gouy−Chapman layers, with energy $w(d)$ per unit area:

$$F(d_0, R) \simeq \pi R \int_{d_0}^{\infty} w(d)\, \mathrm{d}d$$

Using the last equation and eq 51 for $d_0 \ll r_D$ we find

$$F(d_0, R) \simeq \frac{\pi^2}{2}\frac{R}{l_B}\ln\frac{r_D}{d_0}$$

The activation energy F^* corresponds to the minimum (cutoff) $d_0 \sim h_{GC}$:

$$F^* \simeq \frac{\pi^2}{2}\frac{R}{l_B}\ln(2\pi l_B \sigma \alpha r_D) \quad (52)$$

Figure 4. (a) Two spherical aggregates just touching each other. (b) The aggregates develop fwo fingers approaching each other.

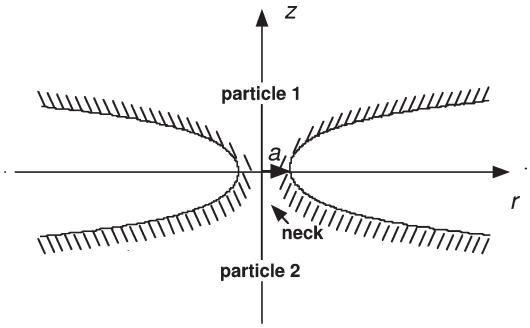

Figure 5. Two aggregates connected by a neck of size a; the neck is characterized by the zero-mean-curvature surface, eq 56.

For $\sigma\alpha \sim 0.3\ \mathrm{nm}^{-2}$ and $r_D \sim 3$ nm we get $F^* \approx 10R(k_BT/\mathrm{nm})$. Therefore, $F^* \gtrsim 30(k_BT)$ for droplets of radius $\gtrsim 3$ nm; that high activation barrier is certainly enough to stabilize the droplet system for 24 h (as can be verified by estimating the droplet collision rate).

6.3. Deformable Aggregates. In the previous section we implicitly assumed that the droplets (peptide aggregates) are spherical and cannot be deformed. This approximation is lifted in the current section. The picture of undeformable spherical aggregates approaching each other is of course justified if the aggregates are rigid (solid-like). However, in this paper we assume that rather the aggregates are liquid-like. In this case the state when two aggregates just touch each other (Figure 4a) is not the proper activation state for their fusion. There are two reasons supporting this statement:

(1) The opposite surfaces of the merging aggregates can be deformed, for example, like it is shown in Figure 4b: rod-like protrusions are emerging toward each other from the aggregates' surfaces. The energy of electrostatic repulsion can be strongly reduced if the protrusions are long enough; simultaneously, the surface area and energy increments can be made however small if the protrusions are thin. (We neglect the bending energy contribution in this argument.)

(2) The state with point-like contact between the aggregates is not exactly relevant: the fusion process requires formation of a neck with finite thickness between the aggregates (Figure 5). As the neck thickness is increased, the free energy first increases, then starts to decrease after reaching the critical state. As it is shown below, the neck contribution to the activation energy barrier is expected to be particularly high in the regime of high surface tension γ in accordance with the fact that the aggregates with high γ are reluctant to change their optimal spherical shape. Note that it is the effective surface tension γ defined in eq 46 that is relevant in this section; γ can be close to γ_0 in the weak charge regime, $\alpha \ll 1$.

Let us consider the activation state of two aggregates connected by the critical neck. The thermodynamic potential is stationary at this critical state implying mechanical (static) equilibrium of the peptide system, in particular, of its surface. There are 3 main forces acting on a surface element (per unit area): (1) the electrostatic force τ; (2) the capillary force $f_{cap} = \gamma C$, where $C = C_1 + C_2$ is the sum of the principal curvatures of the surface; (3) the excess pressure Π inside the aggregate. The force balance (along the surface normal, the positive direction being chosen toward the condensed phase) reads:

$$\tau + \gamma C = \Pi \tag{53}$$

where $\Pi = \mathrm{const}$. This equation defines the aggregate's surface shape for the activation state. As it is shown below, the characteristic neck size a is typically comparable with the Debye length, $a \sim r_D$. In what follows we consider sufficiently large aggregates, $R \gg r_D$. In this case, $\Pi \simeq 2\gamma/R$ since τ is negligible far from the contact region between the aggregates while $C \simeq 2/R$ there.

Let us focus on the region $r \gg a$ (see Figure 2; r is the distance to the vertical z-axis) where the opposite surfaces are nearly parallel. The force τ in this region is defined in eq 50 with $d = 2z$, where $z = z(r)$ defines the upper branch of the surface ($z = 0$ is the symmetry plane cutting the neck in the middle; r,z are cylindrical coordinates). In particular,

$$\tau \sim \frac{k_BT}{l_B r_D{}^2}$$

for $z \sim r_D$. It is shown below that $a \sim r_D$ is the main characteristic length-scale of the neck. This natural length scale can be used to define the dimensionless curvature $\bar{C} = Cr_D$. Using eq 53, we find

$$\bar{C} - \frac{2r_D}{R} \sim -\frac{k_BT}{l_B r_D \gamma} \tag{54}$$

The last term in this equation defines the reduced magnitude of electrostatic repulsion. Below we consider the regime of weak repulsion, $\tau \ll \gamma/r_D$

$$\Gamma \equiv \frac{\pi}{8}\frac{l_B r_D \gamma}{k_BT} \gg 1 \tag{55}$$

This condition is valid if γ is not too low, or if r_D is long enough. It also ensures that the bending energy can be neglected. In fact, the bending energy per unit area is $F_{bend} \sim K_1 C \sim K_1/r_D$, and $K_1 \sim \gamma_0\Delta$. Hence, the condition $F_{bend} \ll \gamma$ is nearly equivalent to $\Gamma \gg 1$ (if

$$\gamma_0 \sim \frac{k_BT}{l_B\Delta}$$

which is roughly the case for the peptide system we consider). Equation 54 thus shows that the reduced curvature is low, $|\bar{C}| \ll 1$, in the regime, condition 55 (recall also that $R \gg r_D$). Therefore, the neck can be approximated by a saddle-like surface of zero mean curvature, $C \equiv 0$. Assuming the axial symmetry (i.e., that $z = z(r)$), we thus arrive at the following surface shape:[23]

$$r \simeq a\cosh(z/a) \tag{56}$$

Below we argue that this equation is applicable everywhere (rather than merely for the neck region, $r \sim a$) in the limiting case $R \to \infty$. To see this let us consider the far region, $r \gg a$. In this case eq 56 can be approximately rewritten as

$$z \simeq a\ln(2r/a),\ r \gg a \tag{57}$$

Let us see whether this shape can be derived using the force balance, eq 53, which, for $r \gg a \sim r_D$, $z \gg a$ (and $R \to \infty$), can be represented as $C = -\tau/\gamma$ with

$$C \simeq \frac{1}{r}\frac{\mathrm{d}}{\mathrm{d}r}\left(r\frac{\mathrm{d}z}{\mathrm{d}r}\right), \quad \tau = \tau(2z) \simeq \frac{k_\mathrm{B}T}{l_B}\frac{8}{\pi {r_D}^2}\,\mathrm{e}^{-2z/r_D}$$

We thus arrive at the following equation

$$\frac{1}{r}\frac{\mathrm{d}}{\mathrm{d}r}\left(r\frac{\mathrm{d}z}{\mathrm{d}r}\right) = -\frac{1}{\Gamma r_D}\,\mathrm{e}^{-2z/r_D} \tag{58}$$

This equation can be also obtained by minimization of the relevant energy $F = G_s + F_{int}$, where

$$G_s = \gamma A_{ex} \simeq \gamma\frac{1}{2}\int_{r_\mathrm{min}}^{r_\mathrm{max}}\left(\frac{\mathrm{d}z}{\mathrm{d}r}\right)^2 2\pi r\,\mathrm{d}r \tag{59}$$

is the excess surface energy (A_{ex} is the excess surface area), and

$$F_{int} = \frac{1}{2}\int_{r_\mathrm{min}}^{r_\mathrm{max}} w(2z)2\pi r\,\mathrm{d}r \tag{60}$$

is half the interaction energy (the other half must be formally attributed to the lower surface branch with $z < 0$). Here

$$w(d) = \frac{k_\mathrm{B}T}{l_B}\frac{8}{\pi r_D}\mathrm{e}^{-d/r_D} \tag{61}$$

is the energy of electrostatic interactions per unit area (see eq 51). The upper limit of integration in eqs 59, 60 is the cutoff length r_{max}. The boundary condition corresponding to the minimum of F is simply

$$\frac{\mathrm{d}z}{\mathrm{d}r} = 0 \qquad \text{at } r = r_\mathrm{max} \tag{62}$$

In order to solve eq 58, we change variables: $(r, z) \to (t, \zeta)$,

$$r = r_D\sqrt{\Gamma}\mathrm{e}^t, \quad z = r_D(t + \zeta) \tag{63}$$

This yields

$$\frac{\mathrm{d}^2\zeta}{\mathrm{d}t^2} = -\mathrm{e}^{-2\zeta}$$

The latter equation is equivalent to the following "conservation law":

$$\left(\frac{\mathrm{d}\zeta}{\mathrm{d}t}\right)^2 = c_0 + \mathrm{e}^{-2\zeta}$$

where c_0 = const is a parameter. The constant c_0 can be obtained imposing the condition 62 and then taking the limit $r_{max} \to \infty$ (which is consistent with $R \to \infty$). Thus, we get: $c_0 = 0$. Hence

$$\frac{\mathrm{d}\zeta}{\mathrm{d}t} = \mathrm{e}^{-\zeta}$$

and

$$\zeta = \ln(t + c_1) \tag{64}$$

where c_1 = const. Introducing the lower bound $r_{min} \sim a$ and demanding that $z \sim a$ at $r = r_{min}$ we find $t_\mathrm{min} \simeq -{}^1/_2\ln\Gamma$ and $c_1 \sim \sqrt{\Gamma}$. Hence, $\zeta = \ln(t + c_1) \simeq {}^1/_2\ln\Gamma = \text{const}$ for $t \ll c_1$, i.e. for $r_\mathrm{min} \ll r \ll r_\mathrm{c} \sim r_\mathrm{D}\mathrm{e}^{\sqrt{\Gamma}}$. The range $r_{min} \ll r \ll r_c$ is exponentially wide since $\Gamma \gg 1$. Using eqs 63, 64 we get in this range

$$z \simeq r_D\left(\ln\frac{r}{r_D} + \text{const}\right), \; r \gg r_\mathrm{D} \tag{65}$$

which is consistent with eq 57. Hence

$$a \simeq r_D, \; r_{max} \to \infty \tag{66}$$

Therefore, the neck shape is indeed defined by the zero-mean-curvature surface, eq 56. This approximation certainly remains valid if the upper cutoff length r_{max} is finite, $r_{max} \gg r_\mathrm{D}$. In this case both the neck energy F_{neck} and the neck radius a can be obtained by the minimization of $F_{neck} = 2(G_s + F_{int})$ with respect to the parameter a (the factor of 2 in the last equation accounts for two equivalent parts of the system, with $z > 0$ and $z < 0$). The free energy F_{neck} is calculated using eqs 59, 60, where the precise value of the lower cutoff $r_{min} \sim a$ is unimportant since the lion's share of the integrals comes from the region $r \gg r_{min}$. The critical parameters obtained as a result are

$$a^* \simeq r_D\left[1 - \frac{1}{2}\frac{\ln\Gamma}{\ln(r_\mathrm{max}/r_D)}\right] \tag{67}$$

$$F^*_{neck} \simeq 2\pi\gamma {r_D}^2 \ln\frac{r_\mathrm{max}}{r_D}\left[1 - \frac{1}{2}\frac{\ln\Gamma}{\ln(r_\mathrm{max}/r_D)}\right]^2 \tag{68}$$

where "$*$" marks the activation state (note that although F^*_{neck} is a minimum with respect to the parameter a, it corresponds to a saddle point in the space of all parameters defining the neck shape). Eqs 67, 68 are valid if

$$r_\mathrm{max}/r_D \gg \sqrt{\Gamma} \tag{69}$$

Let us turn to the general case of finite aggregate radius R, $R \gg r_D$. In this case the general eq 53 is applicable, i.e. $C = -\tau/\gamma + 2/R$. Then eq 58 must be modified as

$$\frac{1}{r}\frac{\mathrm{d}}{\mathrm{d}r}\left(r\frac{\mathrm{d}z}{\mathrm{d}r}\right) = -\frac{1}{\Gamma r_D}\mathrm{e}^{-2z/r_D} + \frac{2}{R}$$

For small r the solution to this equation is $z = z_0 + \delta z$, where z_0 corresponds to $R \to \infty$ and is defined in eq 65, and $\delta z \simeq r^2/2R$ is a perturbation. The unperturbed solution $z = z_0$ is applicable if

$$\frac{\mathrm{d}}{\mathrm{d}r}(\delta z) \ll \frac{\mathrm{d}z_0}{\mathrm{d}r}$$

and $\delta z \ll r_D$. Both conditions are equivalent to $r \ll r_{max}$ with

$$r_\mathrm{max} = \sqrt{Rr_D} \tag{70}$$

For $r \gg r_{max}$ the surface shape becomes nearly spherical:

$$z \simeq \frac{r^2}{2R} + \text{const}, \quad r_\mathrm{max} \ll r \ll R$$

The electrostatic interaction is exponentially weak in this region. It is easy to show that the region $r \gtrsim r_{max}$ provides a subdominant contribution to the excess neck energy, hence

the latter is defined in eq 68 with the cutoff r_{max}, eq 70, obtained above:

$$F^*_{neck} \simeq \pi\gamma {r_D}^2 \ln\frac{R}{r_D}\left[1-\frac{\ln\Gamma}{\ln(R/r_D)}\right]^2 \quad (71)$$

The corresponding critical neck radius is:

$$a^* \simeq r_D\left[1-\frac{\ln\Gamma}{\ln(R/r_D)}\right] \quad (72)$$

Eqs 71, 72 are valid for large enough aggregates, $R \gg \Gamma r_D$ (cf. eq 69).

6.4. Discussion of Results on Fusion of Liquid-Like Aggregates. I. It is the renormalized (effective) surface tension γ (defined in eq 46) including the effect of electrostatic interactions in the Gouy−Chapman layer that is involved in eq 71. The parameter Γ is proportional to γ, therefore the neck radius $a = a^*$ decreases as the surface tension γ is increased. On the other hand, the neck activation energy $F^* = F^*_{neck}$ increases with γ.

II. An increased amphiphilicity of unimers (peptide molecules) leads to lower surface tension γ, hence to lower activation energy for fusion $F^* = F^*_{neck}$, i.e. to weaker kinetic stabilization. On the other hand, as γ drops below 0, finite aggregates become thermodynamically stabilized. It is therefore predicted that the aggregation behavior can change in a nonmonotonic way as the degree of amphiphilicity (the fraction of charged units) is increased: from precipitation at low amphiphilicity (too low surface charge) to kinetically stabilized finite aggregates (moderate positive γ), then to precipitation again (low positive γ), and then to thermodymically stable finite aggregates (negative γ).

III. The results are valid provided that the Gouy−Chapman length h_{GC} is smaller than the Debye length: $h_{GC} \ll r_D$, i.e.

$$\sigma\alpha \gg \frac{1}{2\pi l_B r_D}$$

This is not a strong condition for the surface charge; essentially it demands that r_D is sufficiently long, i.e. that ionic strength is not too high. Using eqs 49, 34 this condition can be represented as (for cation size $\delta \lesssim 5$ Å)

$$I_\infty \lesssim 10^{2(\mathrm{pH}-8)}[\mathrm{M}]$$

which is possibly true if pH $\gtrsim$ 16/3.

IV. Equation 71 shows that the kinetic stabilization of finite aggregates with charged surface can be always achieved if either r_D or γ are sufficiently large. A long-term stability (on the time-scale of days) of nanoaggregates is ensured if the activation energy for their fusion $F^* \gtrsim 30\ k_B T$.[35] Such high F^* is achieved with $\gamma r_D^2 \gtrsim 10\ k_B T$; for $r_D \gtrsim 3$ nm (this corresponds to a wide pH range, 2 < pH < 12 without salt) this is true if $\gamma \gtrsim 4.5$ dyn/cm $\sim 0.1\gamma_0$, which is likely to be the case.

V. So far we neglected the energy of the van der Waals attraction which reduces the activation barrier for fusion:

$$F^* = F^*_{neck} + F_{vdW}$$

For the deformed spherical aggregates connected by the critical neck, the negative van der Waals energy is

$$F_{vdw} \sim -\frac{A}{6}\frac{R}{r_D \ln(R/r_D)}$$

where A is the Hamaker constant (typically $A \sim 1\ k_B T$ for organic particles in water). For $R \sim \Gamma r_D$ this energy, F_{vdW}, is negligible (as compared with F^*_{neck}) if $r_D \gg l_B$. This condition is satisfied for $r_D \gtrsim 3$ nm since $l_B \simeq 0.7$ nm.

VI. The general result that the critical neck radius a is comparable with r_D can be qualitatively explained in the following way: There are two contributions to the neck energy: G_s due to the excess surface area, and F_{int} due to electrostatic interactions. G_s is roughly proportional to a^2. Equations 60, 61, 57 show that $F_{int} \propto {r_{max}}^{2-2a/r_D}$. Therefore, F_{int} is small for $a > r_D$, while G_s is increasing with a in this region. On the other hand, F_{int} gets very large for $a < r_D$, hence the optimum must correspond to $a = a^* \sim r_D$. In a similar manner one can show that the neck energy for $a = a^*$ is dominated by the surface area contribution G_s; more precisely, $G_s/F_{int} \simeq \ln(r_{max}/r_D)$ for $a = a^*$.

VII. We therefore find four conditions necessary for kinetic stabilization: (i) $l_B r_D \gamma \gg k_B T$; (ii) $r_D \gtrsim l_B$; (iii) $r_D \gg h_{GC}$; (iv) $\pi\gamma {r_D}^2 \gtrsim 30 k_B T$. The last condition (iv) essentially follows from conditions i and ii. Condition iii is not too restrictive (see point III above). The main conditions are therefore i and ii.

7. Discussion and Conclusions

1. Aggregation is solutions of oligopeptides is considered theoretically in the present paper. Each peptide molecule consists of n_H hydrophobic (Ala) units and $n_P \ll n_H$ charged hydrophilic (Asp) units. In section 3.1, we argue that charged Asp units strongly prefer to be located at the surface of a peptide aggregate. This is in accordance with the well-known fact that charged Asp residues in proteins are almost exclusively found at the surface of protein globules. We show that the amphiphilic peptides can self-assemble in micelles of different geometries (spherical, cylindrical, plane layer, or vesicle). The following main parameters defining the morphology of peptide aggregates are identified: the length of hydrophilic "block" $m = n_P/n_{Pb}$; the degree of hydrophobicity of the H-units (Ala-units in the present paper) which can be quantified by the H/water interfacial tension γ_0; the H-tail cross-section A_1; the cation size δ. The present theory shows (see section 5) that an increase of m or δ shifts the equilibrium morphology toward the spherical micelles, while an increase of γ_0 or A_1 shifts it to the bilayer membrane structure.

2. The micelles are stabilized primarily by the charged (Asp) units that accumulate at the interface between hydrophobic peptide core and water. The mean charge per hydrophilic (Asp) aminoacid residue depends on pH and ionic strength I_∞ of the solution. Weakly charged micelles are normally not stable thermodynamically: they tend to precipitate as the homogeneous peptide macro-phase has lower free energy than an ensemble of micelles. The main driving force for the peptide precipitation is related to the effective surface tension γ of peptide particles (see eq 46). Macroscopic phase separation of peptides is predicted for $\gamma > 0$; equally sized micelles are stable if $\gamma < 0$. It is found that micelles are stable against aggregation if $I_\infty 10^{pH}$ exceeds a certain threshold (see eq 43) depending on pK for protonation of COO^- group of Asp unit, cation size δ, the energetic affinity ε_P of a neutral Asp for the aqueous environment, and the hydrophobic core surface tension γ_0. The threshold increases with pK, δ and γ_0, and it decreases with ε_P.

3. Four AspAla peptide structures (see Figure 1) with different positions of hydrophilic units in the molecule, but with the same numbers n_H, n_P of Ala and Asp units, are considered. It is found that the double-tail peptide (P3) have the strongest tendency to form flat membranes (or vesicles), the head−tail peptide (P2) rather tends to form cylindrical or spherical micelles, and the peptides P1, P4 (with Asp units separated by Ala-fragments) show an intermediate behavior. For example, for $\delta = 3$ Å and $\gamma_0 = 45$ dyn/cm, it is predicted that P2-peptides self-assemble in spheres of radius $R \approx 2.8$ nm, P3-peptides form layers of

thickness $H \approx 1.9$ nm, and P1 and P4 peptides in the same conditions are close to the boundary between membrane and filament morphologies.

4. The approximation regarding the chain elastic energy F_{el} described at the end of section 2.2 is directly applicable to P2 peptides. In the case of, say, P1 peptides with Asp end-units located close-by at the core surface, the Ala block, which is stretched away from the surface, has to form a hairpin with a sharp U-turn near the middle (where the chain direction is reversed). Such turns are common in protein globules (they are known as reverse turns or β-bends); the β-turns normally involve just four aminoacid units and are stabilized by internal H-bonds.[1] It seems plausible to assume that reverse turns in Asp-Ala peptide micelles and protein globules must be similar. Each turn increases the free energy of the system by some energy E_β. However, this energy penalty can be avoided for P1 peptides by placing their Asp ends at the opposite core/water interfaces in the case of layer morphology, or at the opposite (or distant) points of the cylindrical or spherical surface. Thus, the reverse turns can be disregarded for all the peptides studied here as they nearly does not change the balance between different micellar morphologies (P1 and P2 peptides need not form such turns at all, while each P3 peptide has to form one U-turn near the surface, and each P4 peptide forms 2 U-turns, one near the surface and one in the middle of Ala-block connecting its Asp units).

5. A micelle formation starts above a certain critical concentration (CMC) if the hydrophobic fragments are long enough. The CMC decreases at lower pH (before micelles transform to a macro-segregated peptide phase); CMC always increases with the cation size δ, and CMC strongly decreases with the ionic strength I_∞. The critical micelle concentrations for P1 and P4 peptides (with Asp units separated by Ala-fragments) are predicted to be significantly higher than CMC for P2 and P3 peptides (with Asp dimers).

6. The present theory involves a few essential molecular (n_H, n_P, $m = n_P/n_{Pb}$, A_1, pK) and solution (pH, I_∞, δ, T) parameters, and as such is rather universal: it can be applicable not only to AspAla two-letter peptides, but also more generally to aggregation of amphiphilic molecules (oligomers or short polymers) consisting of two types of units: mainly hydrophobic (H) units, and a small fraction of charged (P) units. For example, Asp (or Ala) units can be replaced by other charged (or, respectively, hydrophobic) aminoacid units.

7. The theory is based on the assumption that hydrophobic core of a peptide aggregate (micelle) is amorphous (liquid-like). There is no general proof of this ansatz. It is well-known that peptides often tend to form regular structures, in particular crystalline or pseudocrystalline structures, stabilized by multiple hydrogen bonds. The assumption of amorphous core is primarily dictated by the logic of the theoretical development: self-assembly of charged amphiphilic molecules (like peptides or copolymers) is a very complicated process, governed by many factors (in particular, the electrolyte effects) apart from the core structure, and the role of these factors is assessed in the present theory. The effects of the secondary or tertiary core structure come on the top of the electrolyte effects, and, in our opinion, must be studied separately.

Is the theory of the present paper directly applicable to real $Ala_{24}Asp_2$ peptide systems? The answer is yes and no. Biologically inspired chirally pure peptides are likely to form regular H-bond structures provided the chains are long enough, so it is a matter of an experimental verification if such structures are formed for peptides with $n_H = 24$ Ala-units aggregated from aqueous solution. If yes, then the core free energy (the energy ε_H gained by an Ala unit upon aggregation) must certainly depend on the micelle morphology. While a regular hydrogen-bond-assisted structure is, in principle, compatible with any core geometry, the strongest (perhaps, pseudocrystalline) core structure is expected for bilayer micelles where hydrophobic molecular fragments can be arranged in parallel arrays (parallel arrangement of Ala-strands favors β-sheet structure). Hence, a higher effective energy ε_H may be expected for the layered structures. The peptide membranes must be strongly favored over other micelle geometries in this case.

On the other hand, the amorphous core assumption is likely to be valid for *achiral* peptides synthesized based on a racemic mixture of aminoacids. In would be therefore extremely interesting to experimentally study self-assembly of achiral peptides complementing it by a parallel study of their chiral analogues (with otherwise the same chemical structure). Such study would permit to elucidate the roles of the core-structure-effects and other (electrolyte) effects separately (not to mention that it would help to advance the theory).

8. While it is predicted that peptide aggregates are not stable thermodynamically in the weak-charge regime, finite peptide particles can still be kinetically stabilized due to electrostatic repulsion of their surface charged groups. We consider kinetic stabilization of two types of peptide aggregates: undeformable solid-like (pseudocrystalline or glassy) and liquid-like. The activation energy barrier F^* for fusion of two rigid weakly charged spherical aggregates (see eq 52) is essentially proportional to the particle size R. A lower barrier F^* is predicted in the case of liquid-like aggregates (see eq 71): here the activation energy increases with R in a logarithmic manner: $F^* \propto \ln R$. In addition, the energy F^* is proportional to the effective surface tension γ and to the Debye length r_D. Formally, a fusion of sufficiently large aggregates is always suppressed by the electrostatic repulsion in both cases (rigid and liquid-like aggregates). However, in practice, this stabilization mechanism for liquid-like surface-charged particles can be turned off if the tension γ or r_D are small enough.

9. We thus predict that weakly charged liquid-like peptide aggregates do not grow indefinitely, but rather their growth is arrested when their size R reaches a few r_D provided that $\gamma r_D^2 \gtrsim 10 k_B T$ and that the critical precipitation concentration (CPC) is very low which is true for $n_H \gg 1$ (see eq 47; low CPC ensures that the Lifshitz-Slezov droplet growth mechanism is suppressed).

10. It is shown that the activation state for fusion of two liquid-like peptide aggregates implies formation of a rather thin critical neck between the merging particles. The neck shape is approximately defined by the zero-mean-curvature (hyperbolic-cosine) surface. The neck radius $a = a^*$ is defined in eq 72. It is typically close to the Debye length r_D.

11. The proposed mechanism of kinetic electrostatic stabilization of peptide particles appears to be rather universal, generically valid for systems of amphiphilic molecules (surfactants, copolymers, peptides) bearing charged groups. In the case of liquid-like metastable aggregates the activation barrier for the fusion is inversely proportional to I_∞. Therefore, the kinetic stabilization of finite aggregates could be easily turned on or off by changing the ionic strength.

12. A nonmonotonic aggregation behavior is predicted as, say, pH of the solution is increased. At low pH the surface charge of self-assembling peptide particles is very low (see eq 49), so they precipitate forming a macro-phase. At somewhat higher pH the surface charge increases and the electrostatic stabilization mechanism comes into play as soon as the Gouy−Chapman length h_{GC} becomes smaller than r_D while the effective surface tension γ is still positive and high enough. The surface tension γ becomes very low (being still positive) at even higher pH, so the electrostatic energy barrier for fusion strongly decreases (see eq 71); this leads to almost unlimited peptide precipitation in this regime. Finally, at higher still pH, the tension γ becomes negative (see eq 45) defining the regime of thermodynamically stable micelles.

13. The molecular self-assembly in aqueous solutions of surfactant-like peptides was experimentally studied recently.[36]

The following peptides were considered:[36] (a) Ala_6Asp, (b) Val_6Asp, (c) Val_6Asp_2, and (d) Leu_6Asp_2. All these peptides have the hydrophobic tail−charged head structure roughly corresponding to the structure of P2-peptide considered in the present paper. The phase diagram obtained for the P2-peptide is qualitatively applicable also for a shorter Ala_6Asp_2 peptide. According to this diagram (shown in Figure 2) it is possible that Ala_6Asp_2 peptides form cylinders (for $\delta \sim 1$ Å corresponding to Na^+ cation radius). Note that all the peptides (a−d)[36] are characterized by a parameter θ_{max} which is lower than that for the reference Ala_6Asp_2 peptide since (i) the Val- and Leu-tails of Val_6Asp_2 and Leu_6Asp_2 peptides are more hydrophobic than Ala-tails, hence higher γ_0 and higher σ for these peptides as compared with Ala_6Asp_2 peptide; (ii) n_P is smaller for the other 2 peptides, Ala_6Asp and Val_6Asp, than for Ala_6Asp_2 peptide (recall that θ_{max} increases with n_P). Therefore, the peptides (a−d) may fall in the membrane region $\theta_{max} < 2$. This conclusion is in qualitative agreement with the data[36] showing that similar structures with the basic bilayer motif are formed by all the four peptides (a−d). The bilayer peptide structures can be favored also for other reasons (see point 7 above).

14. We found that peptide micelles are not stable in low-salt conditions: a significant amount of added salt is required for their thermodynamic stabilization. This result is reminiscent of the well-known "salting in" effect for protein globules.[1] Simultaneously, this result shows that strong amphiphilicity of surfactant-like peptides does not guarantee the micelle stability. For example, lone P2-peptides are strongly amphiphilic at pH = 7, no salt conditions (a P2-peptide has hydrophobic Ala-tail and charged Asp-head in aqueous environment), however micelle formation is inhibited at these conditions due to much lower *local* pH near the micelle surface leading to Asp neutralization and precipitation (macrophase separation) of the peptide (see sections 4.2 and 5.3).

15. So far we did not take into account that the terminal groups of a peptide chain can be charged. The theory developed in this paper is directly applicable to AspAla peptides with chemically modified (neutralized) terminal ends (with uncharged C and N termini). Let us turn to an unmodified peptide molecule having a positive charge (NH_3^+ with p$K \approx 9.6$) at one terminus and negative charge (COO^- with p$K \approx 2.3$) at another terminus. A reconsideration of the micelle formation taking into account the end charges yields the same equations but with different n_{Pb}, n_j: now $n_{Pb} = 2,2,3,3$ and $n_j = 2,2,4,4$ for P1, P2, P3, P4 peptides, respectively. The corresponding values of θ_{max} for $\delta = 3$ Å and $\gamma_0 \approx 45$ dyn/cm are $\theta_{max} \approx 2, 2, 1.1, 1.1$. Hence the following micellar morphologies are predicted with end-charges: cylinders for P1 and P2, and layers (membranes) for P3 and P4 peptides. (Instead of cylinders for P1 and P4, spheres for P2, and layers for P3 peptides predicted for the same parameters in the case of no end-charges.)

Acknowledgment. This work was partially supported by the Alexander von Humboldt Foundation, Programme for Investment in the Future (ZIP, W.Paul Award Project "Sequence Design of Functional Copolymers") and by the French ANR grant "DYNABLOCKs". We acknowledge stimulating discussions with A. R. Khokhlov. A.V.S. acknowledges financial support from the Short Visit Grant 2633 of ESF Scientific Programme "Experimental and Theoretical Design of Stimuli-Responsive Polymeric Materials" (STIPOMAT).

References and Notes

(1) Voet, D.; Voet, J. G. *Biochemistry*; Wiley: New York, 1995.
(2) Flyvbjerg, H. *Phys. Rev. E* **1996**, *54*, 5538. *Phys. Rev. E* **1997**, *56*, 7083.
(3) Rafelski, S. M.; Theriot, J. A. *Annu. Rev. Biochem.* **2004**, *73*, 209.
(4) Fandrich, M.; et al. *Nature* **2001**, *410*, 165.
(5) Lim, A.; et al. *Protein Sci.* **1998**, *7*, 1545.
(6) *Prion biology and diseases*; Prusiner, S. B., Ed.; CSHL Press: New York, 1999.
(7) Stella, L.; Mazzuca, C.; Venanzi, M.; Palleschi, A.; Didone, M.; Formaggio, F.; Toniolo, C.; Pispisa, B. *Biophys. J.* **2004**, *86*, 936.
(8) Aggeli, A.; Nyrkova, I. A.; Bell, M.; Harding, R.; Carrick, L.; McLeish, T. C. B.; Semenov, A. N.; Boden, N. *Proc. Natl.Acad. Sci. U.S.A.* (*PNAS*) **2001**, *98*, 11857.
(9) Aggeli, A.; Nyrkova, I. A.; Bell, M.; Carrick, L.; McLeish, T. C. B.;Semenov, A. N.; Boden, N. In *Self-assembling Peptide Systems in Biology Medicine and Engineering*; Aggeli, A., Boden, N., Zhang, S., Eds.; Kluwer Acad. Publ.: Dordrecht, The Netherlands, 2001; pp 1−17.
(10) Aggeli, A.; Bell, M.; Boden, N.; et al. *Nature* **1997**, *386*, 259.
(11) Aggeli, A.; Bell, M.; Boden, N.; Keen, J. N.; McLeish, T. C. B.; Nyrkova, I.; Radford, S. E.; Semenov, A. *J. Mater. Chem.* **1997**, *7*, 1135.
(12) Aggeli, A.; Bell, M.; Boden, N.; Harding, R.; McLeish, T. C. B.; Nyrkova, I.; Radford, S. E.; Semenov, A. *Biochemist* **2000**, *22*, 10.
(13) Lipowsky, R. *Nature* **1991**, *349*, 475.
(14) Hamley, I. W. *The Physics of Block Copolymers*; Oxford Univ. Press: Oxford, England, 1998.
(15) Nyrkova, I. A.; Semenov, A. N. *Eur. Phys. J. E* **2005**, *17*, 327.
(16) It must be expected that $C^* \sim 1/\Delta$, where $\Delta \sim l_1 \sim 4$ Å is the interfacial thickness. For cylindrical curvature ($C_1 = C$, $C_2 = 0$) C^* can be formally obtained by minimizing F_{bend}, eq 4, with respect to C yielding $C = C^* = \kappa/K$. However, the very quadratic approximation in eq 4 may not be applicable for that high C, so the latter result should be treated as an estimate.
(17) To estimate σ_{max} we approximate an Asp unit by a ball of radius r_P. Its volume

$$V_{1P} = \frac{4\pi}{3} r_P{}^3 = \frac{M_{1P}}{N_A \rho_0}$$

hence $r_P \approx 0.33$ nm, the minimum surface area per Asp is $\pi r_P{}^2$, leading to maximum packing density $\sigma_{max} = 1/(\pi r_P{}^2) \approx 3$ nm^{-2}. This estimate applies to peptides P1, P3, and P4. A twice higher σ_{max} may be expected for P2 since its terminal Asp block can be oriented perpendicular to the surface.
(18) The regime $\sigma^* A_1 > 1$ corresponding to $\theta_{max} < 1$ is not accessible for P1, P2, and P3 peptides since the maximum $\sigma = \sigma_{max}$ is lower than $1/A_1$, see eq. (21).
(19) Kroeger, A.; Deimede, V.; Belack, J.; et al. *Macromolecules* **2007**, *40*, 105.
(20) Kroeger, A.; Belack, J.; Larsen, A.; Fytas, G.; et al. *Macromolecules* **2006**, *39*, 7098.
(21) Bockstaller, M.; Kohler, W.; Wegner, G.; Fytas, G. *Macromolecules* **2001**, *34*, 6353.
(22) Holm, C.; Joanny, J. F.; Kremer, K.; Netz, R. R.; Reineker, P.; Seidel, C.; Vilgis, T. A.; Winkler, R. G. *Adv. Polym. Sci.* **2004**, *166*, 67.
(23) Khokhlov, A. R.; Semenov, A. N.; Subbotin, A. V. *Eur. Phys. J. E* **2005**, *17*, 283.
(24) *Polymer Handbook*, 3rd ed.; Brandrup, J., Immergut, E. H., Eds.; John Wiley and Sons: New York, 1989.
(25) Gouy, G. *J. Phys. Theor. Appl.* **1910**, *9*, 457. Chapman, D. L. *Philos. Mag.* **1913**, *25*, 475.
(26) Pauling, L.; Corey, R. B. *Proc. Natl. Acad. Sci. U.S.A.* **1951**, *37*, 251.
(27) *Polymer Data Handbook*; Oxford Univ. Press: Oxford, U.K.,1999.
(28) www.chemistry.ucsc.edu/courses/palleros/Acids-1.pdf
(29) Rubinstein, M.; Colby, R. H., *Polymer Physics*; Oxford University Press: Oxford, U.K., 2003.
(30) Stern, O. *Z.Electrochem.* **1924**, *30*, 508.
(31) Landau, L. D.; Lifshitz, E. M. *Statistical Physics*; Pergamon Press: Oxford, U.K., 1998.
(32) Israelachvili, J. N.; Mitchell, D. J.; Ninham, B. W. *J. Chem. Soc., Farad.ay Trans. 2* **1976**, *72*, 1525.
(33) Derjaguin, B. V.; Landau, L. D. *Acta Physicochim.* (*USSR*) **1941**, *14*, 633. Verwey, E. J.; Overbeek, J. T. G. *Theory of the Stability of Lyotropic Colloids*; Elsevier: Amsterdam, 1948.

(34) Israelachvili, J. N. *Intermolecular and Surface Forces*; Academic Press: London, 1985.
(35) Napper, D. H. *Polymer Stabilization of Colloidal Dispersions*; Academic: London, 1983.
(36) Vauthey, S.; Santoso, S.; Gong, H. Y.; Watson, N.; Zhang, S. G. *Proc. Natl. Acad. Sci. U.S.A.* **2002**, *99*, 5355.
(37) Levy, Y.; Jortner, J.; Becker, O. M. *Proc. Natl. Acad. Sci. U.S.A.* **2001**, *98*, 2188.
(38) Doruker, P.; Bahar, I. *Biophys. J.* **1997**, *72*, 2445.
(39) Note that certain proteins can form amyloid aggregates with amorphous disordered internal structure instead of native ordered folded structure.[40]
(40) Perutz, M. F.; et al. *Proc. Natl. Acad. Sci. U.S.A.* **2002**, *99*, 5596.
(41) Lee, D.-K.; Ramamoorthy, A. *J. Phys. Chem. B* **1999**, *103*, 271.
(42) Premilat, S.; Hermans, J. *J. Chem. Phys.* **1973**, *59*, 2602.